Diverse organic carbon dynamics captured by radiocarbon analysis of distinct compound classes in a grassland soil

Katherine E. Grant[1*], Marisa N. Repasch[1,2,3], Kari M. Finstad[1], Julia D. Kerr[1], Maxwell Marple[1], Christopher J. Larson[1,4], Taylor A. B. Broek[1,5], Jennifer Pett-Ridge[1,6], and Karis J. McFarlane[1]

[1]Physical and Life Sciences Directorate, Lawrence Livermore National Laboratory, Livermore, CA 94550, USA
[2]Institute of Arctic and Alpine Research, University of Colorado, Boulder, CO, USA
[3]Earth and Planetary Sciences, University of New Mexico, Albuquerque, NM, USA
[4]Department of Earth and Environmental Science, University of Pennsylvania, Philadelphia, PA, USA
[5]National Ocean Sciences Accelerator Mass Spectrometry (NOSAMS) Facility, Woods Hole Oceanographic Institution Woods Hole, MA, USA
[6]Life and Environmental Sciences Department, University of California-Merced, Merced, CA, USA

Correspondence to: Katherine E. Grant (grant39@llnl.gov)

Supplementary Material

1 Density Separation

To fully characterize the soil samples from the Hopland site, we compared the compound class measurements and the physical fractionations to a separate SPT density separation experiment as well as a "bulk" ^{13}C nuclear magnetic resonance (NMR) experiment to compare the change in chemical structure in <2mm soils.

1.1 Methods

Bulk soil samples (~20 g) were density fractionated using a low C and N sodium polytungstate (SPT-O, Geoliquids) into three density fractions: the free light fraction (FLF), the occluded light fraction (OLF), and the dense fraction (DF) according to the method in [*McFarlane et al.*, 2013], The density separation was done in triplicate for each depth sample. The separation density was 1.65 g mL^{-1}. For the experiment all glassware was precombusted to reduce C contamination. For our heavy liquid we used 850 g of SPT powder in 825 g of 18.2 ΩM water in a 1 L beaker and

was constantly stirred using a stir bar. Repeat measurements of the SPT solution ensured the correct density of 1.65 g mL^{-1}.

For each replicate, 20 grams of 2 mm sieved soil from each depth (0-10 cm, 10-20 cm, 20-50 cm, and 50-100 cm) was transferred into an acid-washed centrifuge tube and 100ml of SPT-0, the tube was inverted by hand ensuring the entire sample was in contact with the SPT. The samples were centrifuged at 3500 rpm for 1 hour and the floating material was aspirated and collected via vacuum filtration. Samples were washed repeatedly through a Pall Supor 0.45 mm 47 mm PES filter using 18.2 MΩ water. The FLF was dried in a 65˚C oven overnight, weighed, and then transferred into a 105˚C oven overnight. Once cooled, samples were ground with a mortar and pestle.

To recover the OLF fraction the centrifuge tubes were filled with 75ml SPT. The sample was mixed using a benchtop mixer for 1 minute at 1400 rpm. The sample vial was then transferred into an ice filled Styrofoam box where it cooled for 5 minutes and then sonicated for 1 minute at 80% amplitude. The samples were centrifuged at 3500 rpm for 1 hour to recover the OLF. The floating material (OLF) was then aspirated into a side-arm flask and rinsed five times with about 150 mL of 18.2 MΩ water. The samples were dried at a 65˚C overnight, weighed, and then transferred to a 105˚C oven overnight. The sample was then ground using a mortar and pestle and transferred into vials for later analysis.

The remaining SPT was then aspirated from the centrifuge bottles, leaving just the residual DF. The DF was rinsed until the density of the supernatant reached 1g/ml. The samples were dried in a 65˚C oven overnight, weighed, and then transferred to a 105˚C oven overnight. The DF was grinded using a ball mill and transferred into vials for later analysis.

This entire process was performed in triplicate for each depth; four depths, twelve samples.

As described above, each of the fractions (FLF, OLF, and DF) was loaded into quartz tubes for ^{14}C analysis, and foil balled for $\delta^{13}C$ analysis.

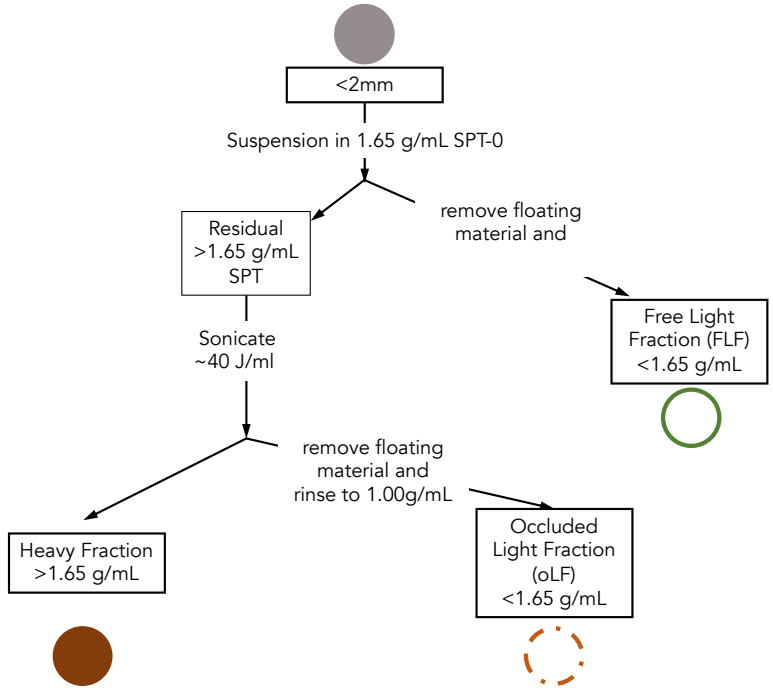

Figure S1: Schematic of density separation work-flow

1.2 Results:

To compare our size fractionated samples to a traditional density fractionation, we carried out the separated our <2mm "bulk soil" into three fractionations with a heavy liquid. The three fractions were the free light fraction (FLF) or mineral free, the occluded light fraction (OLF) is also mineral free, but is found in aggregates and requires disruptive (sonication) energy input, and the dense fraction (DF) is the mineral associated fraction(Plaza et al. 2019). At each depth the FLF was the youngest fraction and hadroughly 26 %OC, the OLF by comparison generally is very condensed with %OC ranging from 32 to 43%. The FLF ranged from +3 ± 5‰ in the surface to -350 ±110‰ at depth. The OLF ranged from 18 ± 7 to -633 ± 21‰. The DF ranged from 14 ± 5 to -563 ± 9‰. In general, the DF was older than both the sand and <63 μm fractions at each

depth, suggesting some modern, mineral-free carbon is present in both the sand and silt/clay fractions. While these separations are not perfect, they help us understand where most carbon is concentrated within a sample. Generally, these HREC soils have very little FLF and OLF by mass, the DF consists of 80% of the total carbon within the sample (SI Table). The HF includes both the sand and silt/clay fractions. Because our >63µm fraction has younger $\Delta^{14}C$ values than the <2mm to >63µm or DF fractions we can assume the <63µm fraction includes free particulate carbon which cycles faster than the truly mineral-associated DF. The OLF is older than both the DF and the FLF at the deepest depth, which could mean aggregation is a mechanism for greater stability in these soils.

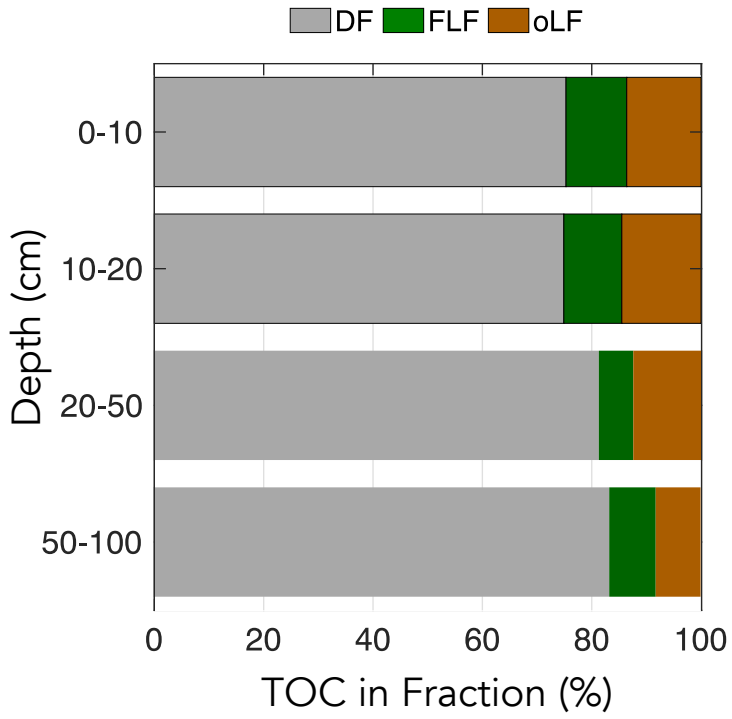

Figure S2. A. Density separation radiocarbon results for the FLF, OLF, and DF.B. fraction of OC contained in each density fraction. Error bars represent standard error on triplicate experiment measurements.

2 Nuclear Magnetic Resonance (NMR) Spectroscopy

2.1 Methods

Semi-quantitative solid-state cross polarization magic angle spinning (CPMAS) ^{13}C NMR was performed on a depth profile of <2mm soil horizon samples to identify target compound classes. In order to reduce paramagnetic iron interferences, soil samples were first de-mineralized using 2% hydrofluoric acid (HF) following the protocols of [*Sanderman et al.*, 2017]. Approximately 0.5 g of de-mineralized soil was crushed into a fine powder with an agate mortar and pestle and loaded into a 7.5mm rotor for NMR analysis. ^{13}C-NMR spectra were collected on a Bruker Neo console operating at a Larmor frequency of 75.71 MHz and externally referenced to adamantane (δ=38.48 ppm). ^{1}H-^{13}C cross polarization measurements were collected while spinning at 6 khz with a contact time of 1ms and a recycle delay of 2s. Spectra were acquired with between 115518 and 346996 scans depending on sample organic carbon concentration. Spectral intensity was normalized by mass and number of scans in Matlab. This method allows for direct comparison between the spectra measured with the same parameters. Spectra were processed with Bruker Topspin software and peak integrations were done with Matlab (vR2022b). Data was categorized by the following functional group shifts: 210-165 ppm, 165-145 ppm, 145-95 ppm, 95-52 ppm, 52-0 ppm, which correspond to C=O groups, aromatic C-O groups, other aromatics and olefinics, O- and N-alkyl groups, and alkyl carbon groups respectively [*Baldock et al.*, 2004; *Mao et al.*, 2017].

2.2 Results:

NMR spectra and total soil organic carbon content were collected from< 2 mm hydrofluoric acid-rinsed soil samples (Figure 2). Total carbon declined from 3.4% at the surface to 0.2% in the 50-100cm interval, with the steepest decline between the 0-10 and 10-20cm intervals. The normalized relative abundances of the five molecular classes we identified by ^{13}C-NMR are listed in Table 1. Generally, the magnitude of all peaks decreased between the surface and subsurface soils, and the 50-100 cm depth had no detectable peaks over baseline. The aromatic peak had the least decline within the sample set, with over 60% of the initial peak intensity retained throughout the depth profile. By comparison, the 20-50 cm depth had >75% less alkyl C relative to the surface soil. We note that the radiocarbon values between the de-mineralized (hydrofluoric acid-rinsed) soils and bulk soils indicate a slightly older value in the de-mineralized soil (SI Table 1), which suggests that some younger, highly labile carbon was removed during this procedure.

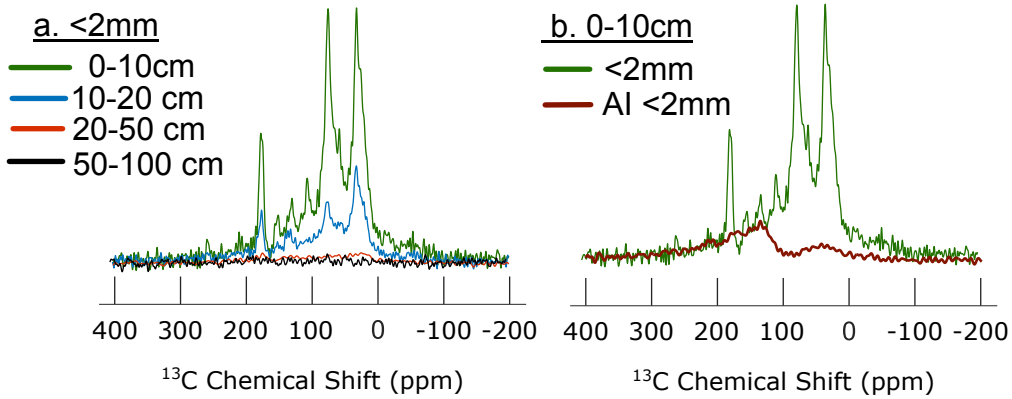

Figure S4: (A) Soil state ^{13}C-NMR and characterization of bulk (< 2 mm) hydrofluoric acid-treated soil collected from four depths of an annual grassland in Hopland, CA. Total organic

carbon was calculated separately on three physical size fractions at each depth. (B). Direct comparison of NMR from AI fraction and bulk soil.

3.1 Radiocarbon Blank Assessment Method

To calculate the amount of exogenous C added during WEOC, TLE, and AA extractions, process blanks were carried out independently. Blank analysis for compound specific radiocarbon analysis (CSRA) becomes increasingly important when the extraction preparations are complex and the sample size of the target compound is small [*Sun et al.*, 2020]. We used ^{14}C modern and dead standard materials to quantify the excess C acquired through each extraction procedure. For the acid insoluble fraction and untreated soil samples background corrections, we ran ^{14}C-free coals as is standard at CAMS.

For the TLE extraction, an empty ASE cell was extracted by the same method as the soil samples. A known amount of modern or dead ^{14}C materials was added to the dried down "blank sample" in the quartz tube. This method uses the "indirect blank" calculation, using a comparison of fraction modern ($F^{14}C$) to an accepted value, because there is not enough excess carbon to measure the blank directly [*Santos et al.*, 2010]. For the AA blank analysis, a ^{14}C-dead alanine powder and a ^{14}C-modern commercial protein powder were digested and processed through the resin column following AA procedures.

In total, three ^{14}C-modern and nine ^{14}C-dead samples were analyzed to quantify the AA blank (SI Table). For the TLE blank quantification, four ^{14}C-modern and four ^{14}C-dead samples were analyzed. The size and $F^{14}C$ of the blank were then determined using the methods and published R script from Sun et al. (2020). The R script was run in R Studio version 4.1.2 (R Core Team, 2021). Briefly, a Bayesian model was used to fit thousands of linear regression lines

between the $F^{14}C$ and inverse of the sample size (1/ μg C), allowing for the calculation of the $F^{14}C$ and size of the blank, as well as their associated uncertainties.

3.2 Radiocarbon blank assessment Results

Extraneous C was quantified for the TLE and AA extractions (SI Table 4). The TLE blank is 8.16 ± 2.54 μg of C with an $F^{14}C$ value of 0.671± 0.252. The exogenous C added from the AA extraction procedure is 11.934 ± 6.205 μg of C with F ^{14}C value of 0.807 ± 0.389. The WEOC blank contribution is 2.818 ± 0.753 with a $F^{14}C$ value of 0.298 ± 1.22 (details reported in Finstad et al., 2023). Generally, the extracted ^{14}C samples were large enough (> 250 μg C) that the contribution of the blank did not significantly shift the ^{14}C values outside the variability of sample replicates. Future efforts will identify the source of extraneous C to lower this blank contribution from materials or a methodology step and increase the applicability of this method for smaller and more ^{14}C-depleated samples.

4 Works Cited

Baldock, J. A., C. A. Masiello, Y. Gélinas, and J. I. Hedges (2004), Cycling and composition of organic matter in terrestrial and marine ecosystems, *Marine Chemistry*, *92*(1), 39-64, doi:https://doi.org/10.1016/j.marchem.2004.06.016.

Mao, J., X. Cao, D. C. Olk, W. Chu, and K. Schmidt-Rohr (2017), Advanced solid-state NMR spectroscopy of natural organic matter, *Progress in Nuclear Magnetic Resonance Spectroscopy*, *100*, 17-51, doi:https://doi.org/10.1016/j.pnmrs.2016.11.003.

McFarlane, K. J., M. S. Torn, P. J. Hanson, R. C. Porras, C. W. Swanston, M. A. Callaham, and T. P. Guilderson (2013), Comparison of soil organic matter dynamics at five temperate deciduous forests with physical fractionation and radiocarbon measurements, *Biogeochemistry*, *112*(1), 457-476, doi:10.1007/s10533-012-9740-1.

Sanderman, J., M. Farrell, P. I. Macreadie, M. Hayes, J. McGowan, and J. Baldock (2017), Is demineralization with dilute hydrofluoric acid a viable method for isolating mineral stabilized soil organic matter?, *Geoderma*, *304*, 4-11, doi:https://doi.org/10.1016/j.geoderma.2017.03.002.
Santos, G. M., J. R. Southon, N. J. Drenzek, L. A. Ziolkowski, E. Druffel, X. Xu, D. Zhang, S. Trumbore, T. I. Eglinton, and K. A. Hughen (2010), Blank Assessment for Ultra-Small Radiocarbon Samples: Chemical Extraction and Separation Versus AMS, *Radiocarbon*, *52*(3), 1322-1335, doi:10.1017/S0033822200046415.
Sun, S., et al. (2020), 14C Blank Assessment in Small-Scale Compound-Specific Radiocarbon Analysis of Lipid Biomarkers and Lignin Phenols, *Radiocarbon*, *62*(1), 207-218, doi:10.1017/RDC.2019.108.